Synthesis of Perpendicular Nanorod Arrays with Hierarchical Architecture and Water Slipping Superhydrophobic Properties

Hye-Mi Bok, Sungwan Kim, Sang-Hoon Yoo, Seong Kyu Kim,* and Sungho Park*

Department of Chemistry, BK21 School of Chemical Materials Science and SKKU Advanced Institute of Nanotechnology, Sungkyunkwan University, Suwon 440-746, South Korea

Received August 31, 2007. In Final Form: November 20, 2007

The utilization of vertically aligned smooth gold nanorod arrays with and without nanoporous tip architectures as superhydrophobic surfaces is described. Nanoporous architecture was produced on the tips of nanorods by selectively dissolving less noble components from the alloy nanorods. The resulting nanoscopic dual-size roughness features enhanced the surface dewettability after surface modification with low-surface-energy materials such as long-chain normal alkanethiols and fluorinated organic compounds. The surface cleaning properties were also tested with a rolling water droplet.

1. Introduction

The wettability of a solid surface is an important scientific and technological topic and attracts a great deal of interest from both practical and fundamental standpoints.[1,2] Special attention has been focused on superhydrophobic surfaces as a result of a variety of practical applications, such as antibiofouling paints for boats,[3] antisticking of snow for antennas,[4] self-cleaning of windshields,[5] and so forth. When a water droplet contacts such a surface, it will form a spherical shape that is often characterized by a contact angle. Surfaces with very high contact angles typically larger than 150° are called superhydrophobic surfaces.[1,2] Given that there are a myriad of examples of superhydrophobic living creatures in nature, such as lotus leaves, a water-strider's legs, and a cicada orni's wings, substantial efforts have been devoted to characterizing such structures and therefore to mimicking their structures and chemistry in order to create superhydrophobic surfaces.[6−18] These surfaces exhibit large water contact angles and show water-repellent properties. This property has often been emphasized as "self-cleaning" or the "lotus leaf effect". In this process, water droplets roll off the surface upon a slight tilting without water spreading on the leaf surface and remove contaminants from the surface. This phenomenon has been explained by forming the large water/air interface below a water droplet, which is induced by the air trapped in pockets of a hierarchically textured surface. Conventionally, this type of surface is described by the Cassie−Baxter model in which the apparent contact angle is expressed by the sum of all the contributions of the different phases, such as water/air and water/solid interfaces.[19] To form such a surface, there are two general common features to be considered. One is micro- and/or nanostructures on the surface. The other is a coating of such micro-/nanostrucutures with low-surface-energy materials. There are many examples of generating rough surfaces, including electrospinning, template methods, chemical etching, chemical vapor deposition, electrodeposition, polymer solution evaporation, and nanorod array growth.[10] For materials of low surface energy, long-chain normal alkane and fluorinated organic compounds are representative examples.[10]

Among recently reported results, metallic superhydrophobic surfaces have attracted a great deal of interest because of their technological importance and easy control of morphology with a variety of fabrication methods.[7] In particular, a forest of slender pillars with sharp tip morphology showed superhydrophobic and water-repellent properties that are important characteristics for designing a low-friction surface for microfluidic channels.[20−22] Herein we describe a new strategy for synthesizing such slender pillars by the electrochemical deposition of metals into nanopores of anodized aluminum oxide (AAO) templates. Although the AAO-mediated nanorod synthesis has been a popular synthesis route for generating a variety of organic and inorganic rod-shaped materials, there has been no example for generating morphology-controlled nanorod arrays by engineering the deposition scheme and therefore characterizing their effect on the resulting surface properties. Our results show that hierarchical nanostructures with double roughness can be readily fabricated by combining electrochemical deposition and chemical etching processes. The double roughness enhances the surface superhydrophobicity and shows a higher contact angle compared to

* Corresponding authors. (S.K.K.) E-mail: skkim@skku.edu. (S.P.) E-mail: spark72@skku.edu.

(1) Sung, T.; Feng, L.; Gao, X.; Jiang, L. *Acc. Chem. Res.* **2005**, *38*, 644.
(2) Feng, X.; Jiang, L. *Adv. Mater*. **2006**, *18*, 3063.
(3) Scardino, A.; De Nys, R.; Ison, O.; O'Connor, W.; Steinberg, P. *Biofouling* **2003**, *19*, 221.
(4) Kako, T.; Nakajima, A.; Irie, H.; Kato, Z.; Uematsu, K.; Watanabe, T.; Hashimoto, K. *J. Mater. Sci*. **2004**, *39*, 547.
(5) Quere, D. *Rep. Prog. Phys.* **2005**, *68*, 2495.
(6) Lim, H. S.; Han, J. T.; Kwak, D.; Jin, M.; Cho, K. *J. Am. Chem. Soc.* **2006**, *128*, 14458.
(7) Bormashenko, D.; Stein, T.; Whyman, G.; Bormashenko, Y.; Pogreb, R. *Langmuir* **2006**, *22*, 9982.
(8) Pacifico, J.; Endo, K.; Morgan, S.; Mulvaney, P. *Langmuir* **2006**, *22*, 11072.
(9) Cho, W. K.; Kang, S. M.; Kim, D. J.; Yang, S. H.; Choi, I. S. *Langmuir* **2006**, *22*, 11208.
(10) Zhang, L.; Zhou, Z.; Cheng, B.; Desimone, J. M.; Samulski, E. T. *Langmuir* **2006**, *22*, 8576.
(11) Shi, F.; Song, Y.; Niu, J.; Xia, X.; Wang, Z.; Zhang, X. *Chem. Mater*. **2006**, *18*, 1365.
(12) Artus, G. R. J.; Jung, S.; Zimmermann, J.; Gautschi, H.-P.; Marquardt, K.; Seeger, S. *Adv. Mater*. **2006**, *18*, 2758.
(13) Chen, H.; Zhang, F.; Fu, S.; Duan, X. *Adv. Mater*. **2006**, *18*, 3089.
(14) Abdelsalam, M. E.; Bartlett, P. N.; Kelf, T.; Baumberg, J. *Langmuir* **2005**, *21*, 1753.
(15) Xu, L.; Chen, W.; Mulchandani, A.; Yan, Y. *Angew. Chem., Int. Ed*. **2005**, *44*, 6009.
(16) Li, Y.; Shi, G. *J. Phys. Chem. B* **2005**, *109*, 23787.
(17) Shirtcliffe, N. J.; McHale, G.; Newton, M. I.; Chabrol, G.; Perry, C. C. *Adv. Mater*. **2004**, *16*, 1929.
(18) Martines, E.; Seunarine, K.; Morgan, H.; Gadegaard, N.; Wilkinson, C. D. W.; Riehle, M. O. *Nano Lett.* **2005**, *5*, 2097.
(19) Cassie, A. B. D.; Baxter, S. *Trans. Faraday Soc.* **1944**, *40*, 546.
(20) Hosono, E.; Fujihara, S.; Honma, I.; Zhou, H. *J. Am. Chem. Soc.* **2005**, *127*, 13458.
(21) Lee, W.; Jin, M.-K.; Yoo, W.-C.; Lee, J.-K. *Langmuir* **2004**, *20*, 7665.
(22) Choi, C.-H.; Kim, C.-J. *Phys. Rev. Lett*. **2006**, *96*, 066001.

10.1021/la7026972 CCC: $40.75
Published on Web 03/01/2008

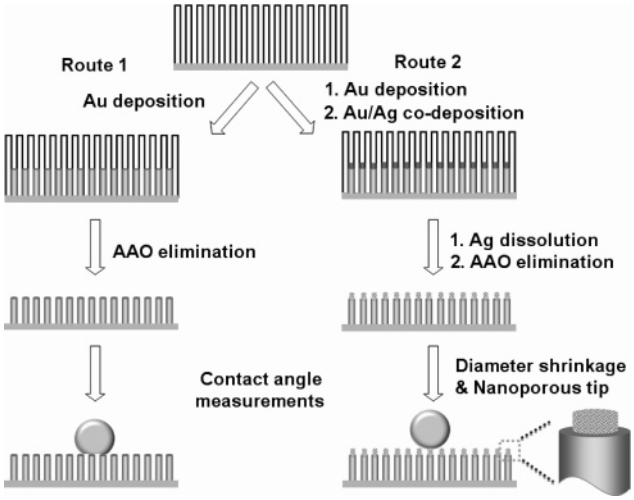

Figure 1. Schematic of the experimental procedure for the synthesis of vertically aligned smooth gold nanorod arrays without (route 1) and with (route 2) nanoporous tips.

analogous structures with single roughness. Although all of the superhydrophobic surfaces do not necessarily exhibit a low-friction property,[23] our resulting slender pillars with nanoporous tips showed a low-friction surface property that is important for self-cleaning and microfluid channel design.

2. Experimental Section

The synthesis of vertical arrays of gold nanorods is based on the AAO template-assisted electrochemical deposition method, which was used in previous examples.[24] In brief, a thin layer of gold (~1 μm) was thermally evaporated on one side of a nanoporous AAO membrane (pore size = 250−350 nm) and served as a working electrode in a three-electrode electrochemical cell after making physical contact with a glassy carbon electrode. A Pt wire and a Ag/AgCl electrode were employed as a counter and a reference electrode, respectively. Next, gold nanorods were electrodeposited into the interior of an AAO template at constant potential, −0.95 V versus Ag/AgCl. Gold/silver nanorods were electroplated with a 1/3 gold/silver ionic ratio prepared from homemade plating solutions (50 mM $KAu(CN)_2$ and 50 mM of $KAg(CN)_2$, Alfa Aesar). AAO membranes were obtained from Whatman International.

The morphology of the resulting nanorods was investigated by a JEOL 7000F field emission scanning electron microscope. The water contact angles on such surfaces were measured using the SEO 300A at ambient temperature. The sliding angle movie clips were obtained with a Canon IXY 600 digital camera. All measurements, except the time-dependent contact-angle measurements, were performed five times, and average values with corresponding standard deviations were obtained.

3. Results and Discussion

In a typical experiment, vertically aligned nanorod arrays were formed by the electrochemical deposition of metals into the interior of an AAO template, and the length of gold nanorods was systematically controlled by monitoring the charge passed during the electrodeposition process (in route 1, Figure 1). In synthesis route 2, a similar procedure was adopted except that gold/silver alloy nanorods were deposited on the tip of predeposited gold nanorods. Gold/silver alloy nanorods were electrodeposited from solution containing gold/silver ions (1/3 mol/mol Au^+/Ag^+) in basic cyanide solutions. Before dissolving the AAO template in 3 M sodium hydroxide solution, the sample was exposed to concentrated nitric acid to dissolve silver from the nanorods selectively. This process induces porous nanorod tip formation due to an intrinsic dynamical pattern-formation process in which the more noble metal (gold) atoms tend to aggregate into 2D clusters by a phase-separation process at the solid−acid interface.[25] During this dissolution process, the gold block not only forms a porous nanostructure but also shrinks its diameter about 35%.

Typical scanning electron microscopy (SEM) images for gold nanorod arrays with different rod lengths synthesized via route 1 are shown in Figure 2(A−C). As shown in the insets, the lengths of the nanorods were systematically increased to 0.42 (±0.04 μm), 1.52 (±0.09 μm), and 12.61 (±0.70 μm), respectively. The average diameter was 300 (±30 nm) for all samples. When the rod length was >5 μm, the nanorods showed a tendency to bundle as a result of attractive forces that arose during the evaporation process and a large internanorod contact area. Therefore, the internanorod distance became shorter as the length increased and was accompanied by the appearance of micrometer-scale crack features between large bundles. When a water droplet (3 μL) was introduced onto the nanorod forest, it seeped into the nanorod forest, and the contact angle decreased consistently as the rod length increased, as shown in Figure 2D−F. Metallic surfaces are well known to have high surface energy, on the order of 1 eV of chemical binding energy, and therefore show liquid spreading of water droplets.[26]

The roughness-dependent contact-angle variation can be understood in the context of the Wenzel model, in which there is a linear relationship between the apparent contact angle and the roughness factor of the surface. It is represented by a simple equation, $\cos\theta_w = r\cos\theta$, where θ_w represents the apparent contact angle, r corresponds to the surface roughness factor, and θ is the intrinsic contact angle.[27] This model states that if θ on a smooth surface is less than 90° then θ_w will become smaller as the roughness increases. This roughness factor (r) increases as the rod length increases in our system. Superhydrophobic metallic surfaces are usually obtained by a monolayer coating of low-surface-energy materials, such as long-chain normal alkane and fluorinated organic compounds. To convert the hydrophilic surfaces into hydrophobic ones, the surfaces of nanorod forests were coated with heptadecafluoro-1-decanethiol (HDFT) by immersion in a 0.01 M toluene solution for 12 h. The resulting contact-angle measurements on such surfaces are represented in Figure 2G−I, corresponding to Figure 2A−C SEM images, respectively. As in the case of hydrophilic surfaces, the contact angle varied as the rod length increased. For a hydrophobic surface (θ > 90°), θ_w on a rough surface became larger as the roughness increased. This trend is clearly evident in our nanorod forest systems.

Of central interest here is the double roughness influence on the contact-angle variation on the nanorod forests, which were generated by following synthesis route 2 in Figure 1. Representative SEM images are shown in Figure 3 A−C. All of the nanorod samples show smooth main body surfaces with corrugated and nanoporous tip architecture accompanied by a contracted diameter. The total lengths of the nanorods were systematically increased to 0.41 (±0.04 μm), 1.48 (±0.07 μm), and 13.23 (±0.91 μm). The porous nanorod tip lengths were fixed to about 200−400 nm for all samples. As in the case of smooth nanorod forests, the contact-angle measurements show a rod-length-dependent variation, following Wenzel's prediction,

(23) Jin, M.; Feng, X.; Feng, L.; Sun, T.; Zhai, J.; Li, T.; Jiang, L. *Adv. Mater*. **2005**, *17*, 1977.
(24) Park, S.; Lim, J.-H.; Chung, S.-W.; Mirkin, C. A. *Science* **2004**, *303*, 348.
(25) Yoo, S.-H.; Park, S. *Adv. Mater*. **2007**, *19*, 1612.
(26) de Gennes, P. G.; Brochard-Wyart, F.; Quere, D. *Capillary and Wetting Phenomena*; Springer: Berlin, 2003.
(27) Wenzel, R. N. *Ind. Eng. Chem*. **1936**, *28*, 988.

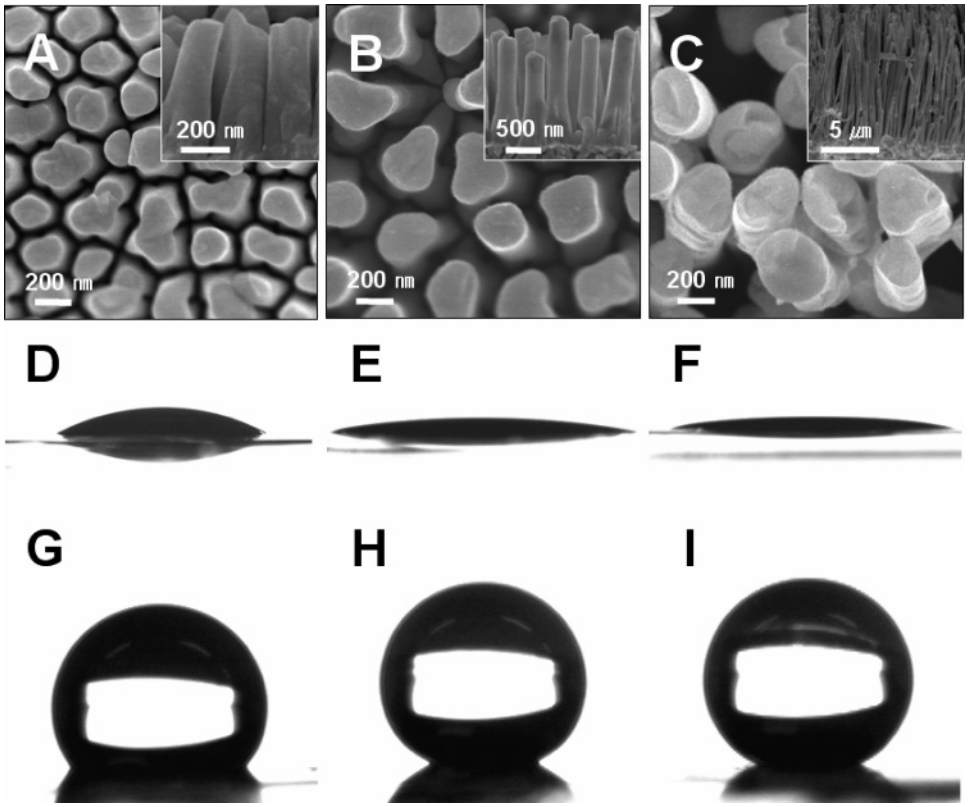

Figure 2. Field-emission SEM images of smooth gold nanorod arrays with different rod lengths (A−C top views). Insets show the corresponding side views. Their corresponding contact-angle measurements are shown without (D−F) and with (G−I) HDFT coatings.

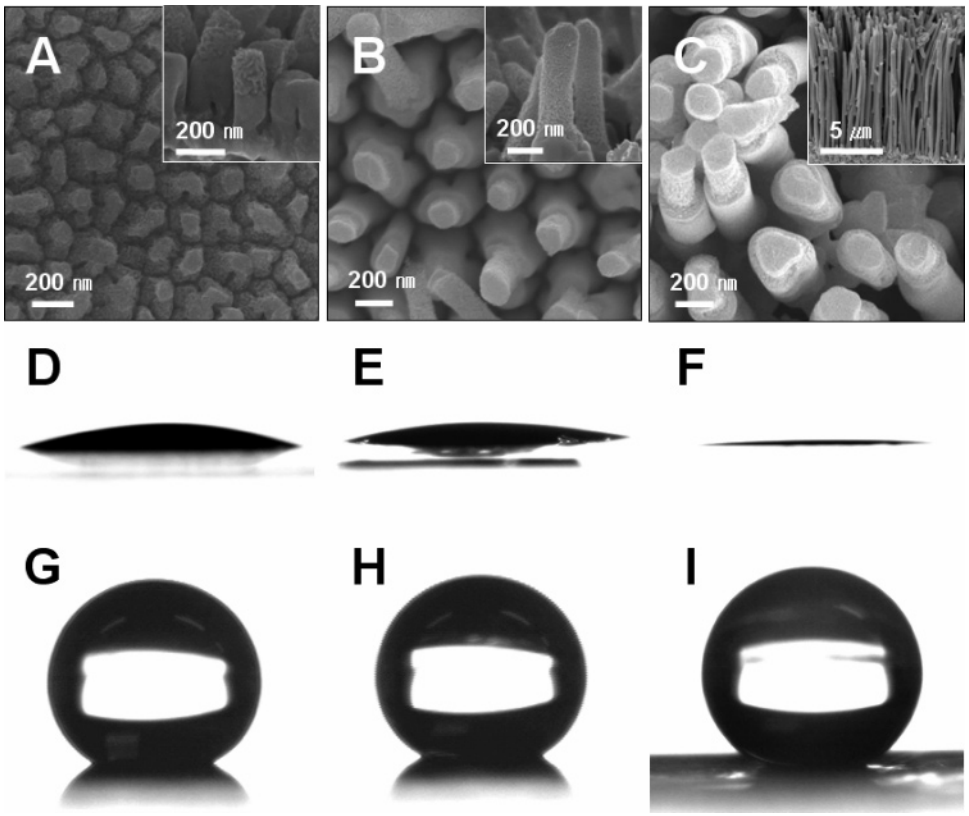

Figure 3. Field-emission SEM images of smooth gold nanorod arrays with nanoporous tips with different rod lengths (A−C, top views). Insets show the corresponding side views. Their corresponding contact-angle measurements are shown without (D−F) and with (G−I) HDFT coatings.

for hydrophilic surfaces of $\theta_w < \theta < 90°$ before surface coating and for hydrophobic surfaces of $\theta_w > \theta > 90°$ after surface coating with HDFT. There was no deterioration of the nanopores after HDFT modification, which was confirmed from SEM images (data not shown). Their contact-angle variations are well illustrated in Figure 3D−F for hydrophilic surfaces and in Figure 3G−I for

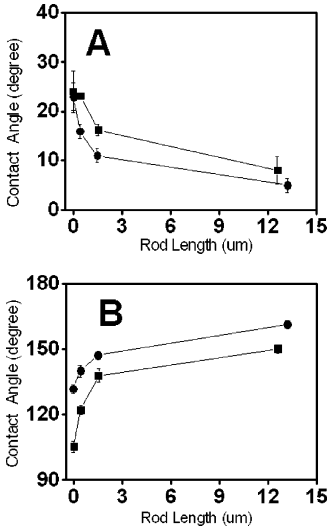

Figure 4. Contact-angle measurements on smooth gold nanorod arrays with (●) and without (■) nanoporous tips. (A, B) Contact angles without and with HDFT coatings, respectively.

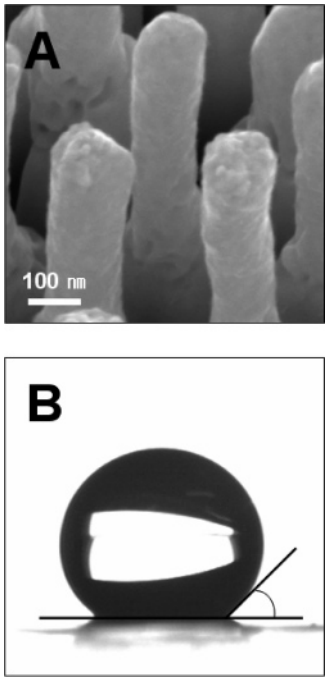

Figure 5. (A) FESEM image of gold nanorod arrays with a shrunken diameter (171 ± 11 nm) after selective electrochemical filling of the nanopores with gold. (B) Corresponding contact angle (135 ± 2°) on the surface.

hydrophobic surfaces. To investigate the influence of nanoporous architecture on contact angles, we carried out a comparison experiment with smooth and nanoporous plain gold plates without nanorod features (Supporting Information, Figure S1). The nanoporosity clearly increased the hydrophilicity and hydrophobicity by following Wenzel's model. The dealloying process generated nanopores ($d \approx 24 \pm 9$ nm, Supporting Information, Figure S2) on the surface and led to an increase in the roughness factor on plain plates. However, the maximum contact angle on a hydrophobic surface was around 130°, and further increases were not obtainable with such a substrate.

Figure 4 shows the contact-angle variation as a function of the lengths of vertically aligned nanorod forests as well as for a plain substrate without any nanorod features. As is clearly evident in Figure 4, there are two noticeable features. First, both hydrophilicity and hydrophobicity increase as the rod length increases. Second, for a given nanorod length, the formation of nanoporous tip at the end of the nanorods enhances the wettability and dewettability before and after surface coating with low-surface-energy materials, respectively. For a smooth nanorod forest without nanoporous tips, a superhydrophobic surface (contact angle >150°) is obtainable when the length becomes larger than 10 μm. However, the nanoporous tip modification allows the contact angle to reach ca. 150° when the length is only around 3 μm. Significantly, the results show that the double-roughness architecture helps to amplify the apparent contact angle, which is consistent with Patankar's recent theoretical analysis.[28] According to his analysis, the double roughness also enhances the water slippage on such structures because of the easy formation of a composite drop with a favorable energy state. Our hierarchical nanostructures show an obvious double roughness. One is a perpendicular array of nanorods, and the other is nanoporous fine structure on the tips of nanorods. It is noteworthy that the contraction of nanorod diameter from the dealloying process alone could not bring the represented contact-angle variation. As shown in Figure 5, we prepared an array of nanorods with a smooth tip surface but retained the contracted diameter by selectively filling the nanopores on the nanorods using the slow electrochemical deposition of gold by 20 cyclings of potential from −0.5 to −0.7 V (vs Ag/AgCl) with a scan rate of 50 mV/s. The diameter was 171 ± 11 nm, and the total length of the nanorods was 1.63 (±0.07 μm). The surface is smoother than the analogous nanoporous tips. The measured contact angle (135 ± 2°) was comparable to the value measured on an array of smooth nanorods (Figure 4B). This comparison experiment confirms that the nanoporous hierarchy nanostructure rather than the diameter shrinkage is mainly attributed to the enhanced hydrophobicity. Previously, the porous architecture of polymer fibers showed enhanced hydrophobicity compared to the architecture of nonporous fibers.[29] Also, Larmour et al. recently reported the importance of dual roughness in enhancing the hydrophobicity.[30] With the given morphology, the addition of the nanoporous architecture probably leads to reducing the surface fraction of the solid/water contact area.

The contact angle of composite water droplets can be described by the Cassie−Baxter (CB) model, which states that the apparent contact angle is the sum of all of the contributions of different phases (e.g., $\cos\theta_c = f(1 + \cos\theta) - 1$, where θ_c represents the apparent contact angle and f and θ correspond to the surface fraction of solid/water and the intrinsic contact angle on the smooth solid surface, respectively).[19] Therefore, the smaller the surface solid fraction, the larger the apparent contact angle (θ_c). Unlike the Wenzel model, the CB model states that when the intrinsic contact angle of a water droplet on a smooth surface is less than 90° the contact angle can still be enhanced by the entrapped air pockets within the textured structures.[2] Our smooth and nanoporous nanorod systems follow the Wenzel model before surface coating with HDFT because the apparent contact angle consistently decreases as the surface roughness increases as a function of nanorod length. However, when nanorods are hydrophobitized by surface coating with HDFT, the CB model plays a critical role in terms of understanding the water slippage. Both the Wenzel and the CB models can explain the contact-angle augmentation with the increase in nanorod length as a

(28) Patankar, N. A. *Langmuir* **2004**, *20*, 8209.

(29) McCann, J. T.; Marquez, M.; Xia, Y. *J. Am. Chem. Soc.* **2006**, *128*, 1436.

(30) Larmour, I. A.; Bell, S. E. J.; Saunders, G. C. *Angew. Chem., Int. Ed.* **2007**, *46*, 1710.

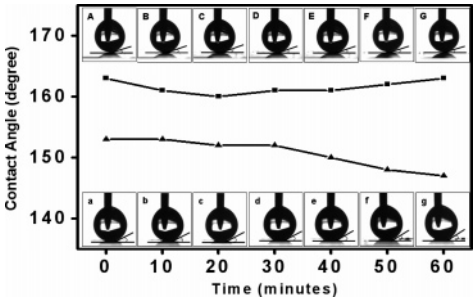

Figure 6. Apparent contact-angle measurement as a function of contact time. Upper images A−G: snap photographs of the contact-angle measurement on the nanoporous nanorod (total length ≈ 1.48 (±0.07 μm)) arrays after the application of a 1-hexadecanethiol coating. The corresponding contact angles are plotted with filled squares. Lower images a−g: the same as in the upper case except that the surface was coated with HDFT instead of 1-hexadecanethiol. The corresponding contact angles are plotted with filled triangles.

result of the roughness increase or air entrapment below the water droplet, respectively.

We have checked the dynamic behavior of contact angles on the array of nanoporous nanorods. The so-called wicking test allows one to investigate the time-dependent contact-angle variation.[31] The contact angles were measured as a function of the contact time between the water droplet and the surface, as shown in Figure 6. The nanoporous nanorods with an HDFT coating showed stable contact angles for 30 min. After this point, the contact angle started to decrease slightly, probably as a result of the pinning of water droplets in the nanopores. However, when we coated the same structure with 1-hexadecanethiols, the contact angle was increased to 162 ± 1° and was very stable during the wicking test. The nanoporous nanorods kept their superhydrophobic characteristics even after the 1 h wicking test and exhibited low surface friction for water droplet rolling.

The water droplet slippage with low surface friction, which is critical for designing self-cleaning surfaces, can be observed with different characteristics. We measured the sliding angles for all samples and found that the long, smooth nanorod forest shown in Figure 2C and the nanoporous nanorod forests shown in Figure 3B,C represent very low sliding angles, typically around 2° for 10 μL water droplets (Supporting Information, movie clips 1−3). In particular, when the rod lengths are comparable, the role of the nanoporous tip is critical for enhancing water droplet roll-off at low sliding angles. This is clearly represented by a lower sliding angle (∼2°) for the nanoporous nanorod forest (L = 1.48 (±0.07 μm), shown in Figure 3B) compared to that for the analogous smooth nanorod forest (L = 1.52 (±0.09 μm), shown in Figure 2B, showing a sliding angle of >15°). We also measured the sliding angles for the nanoporous flat surfaces as a control experiment and found that the nanoporous flat surface represented very high sliding angles, typically >90° for 10 μL water droplets (Supporting Information, movie clip 4). Even the upturned tilting showed the strong sticking characteristics of water droplets on such surfaces.

Usually, contact-angle hysteresis, which is the difference between advancing and receding contact angles, is often utilized to differentiate two models. In the CB model, the contact-angle hysteresis is extremely small, but this value becomes large in the Wenzel model. In the CB model, the low surface energy of air reduces the friction force when a water droplet moves. However, the opposite trend is the resulting phenomenon in the Wenzel model, which favors water droplet pinning and therefore leads

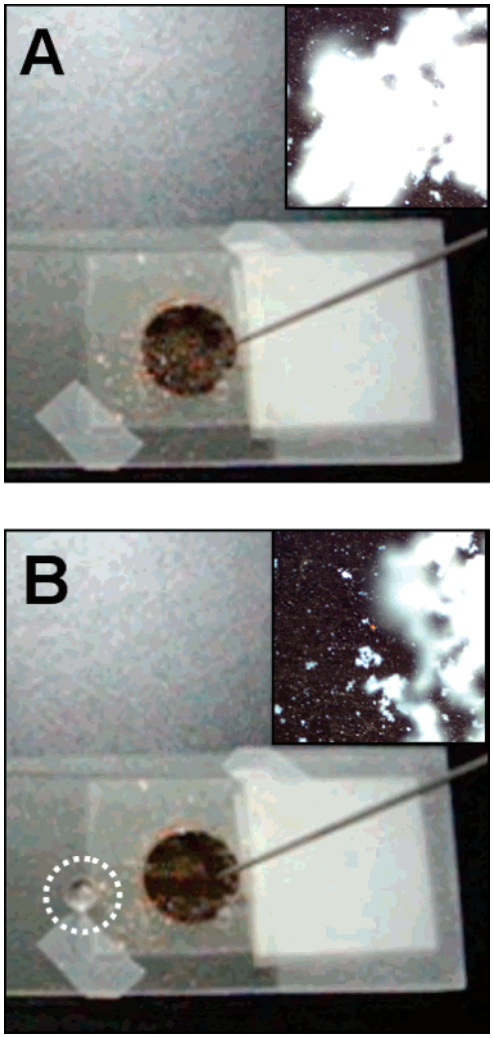

Figure 7. Surface cleaning demonstration with water droplet rolling. Photograph of the surface of nanoporous nanorods contaminated with dust powder (A) before and (B) after water droplet rolling. The dotted white circle emphasizes the water droplet after rolling. The insets show enlarged optical images (×100).

to the increase in frictional force. Therefore, the sliding angle measurement is critical in terms of differentiating two models. When the contact-angle hysteresis becomes smaller, the sliding angle of a water droplet is smaller, which follows the CB model. The quantitative relationship between the contact-angle hysteresis and the sliding angle is given by Furmidge as $mg \sin \alpha = \gamma w(\cos R - \cos A)$, where α is the sliding angle, mg is the weight of the water droplet, w is the diameter of the wetted area, γ is the interfacial tension of the water at the water/air interface, and R and A are the receding and the advancing contact angles, respectively.[32] From this statement, it can be found that a smaller difference between the advancing and the receding contact angles will lead to a smaller sliding angle (α). According to the theoretical simulation, the contact mode can be switched continuously from the Wenzel to the CB mode with increasing surface roughness.[33] As the rod lengths increase, the surface roughness increases, and this effect should convert the Wenzel mode to the CB mode. Special attention needs to be directed to nanoporous nanorod forests. Compared to smooth nanorod forests, the nanoporous nanorod architecture showed enhanced contact angles with low sliding angles. Obviously, the first one of double roughness is

(31) Wu, X.; Zheng, L.; Wu, D. *Langmuir* **2005**, *21*, 2665.

(32) Furmidge, C. G. L. *J. Colloid Sci.* **1962**, *17*, 309.

(33) Quere, D.; Lafuma, A.; Bico, J. *Nanotechnology* **2003**, *14*, 1109.

induced by nanorod arrays, and the second one is endowed by nanoporous architecture, which increases the apparent contact angle. More importantly, it also enhances water rolling on such surfaces. The self-cleaning property was tested by rolling a water droplet on the dust-contaminated nanorod surface. As represented in Figure 7, the surface of nanoporous nanorods where a water droplet had rolled along was cleaned. The inset in Figure 7B shows the optical microscope image ($\times$100) of the surface where the droplet rolled. The white foggy particle was the dust on the surface, and the dark region was the place where the water rolled (Supporting Information, movie clip 5).

Given that internanorod distance and individual rod size can be tuned by the physical dimensions of the template, the controllability of nanorod length and its nanoscopic porosity are variables with which the surface dewettability and water slippage can be further enhanced. The internanorod distance can be tuned by controlling AAO membrane synthesis conditions and the nanoporosity in a nanorod can be tailored as a function of the relative gold/silver ion concentration ratios in a plating solution.

4. Conclusions

The present results show that it is important to design hierarchical double roughness features that not only induce air trapping but also make this state more stable than the Wenzel one. These prerequisites for forming superhydrophobic surfaces without generating sticky surfaces have been suggested by Quere et al.[33] They suggested that the roughness factor r should be made larger than $1/|\cos|$ and therefore air trapping must be favored on these surfaces with appropriate stability. This is achievable by rationally increasing the roughness factor. With the present results, it is clearly evident that the nanoscopic nanoporosity greatly enhances the roughness compared to that of the analogous smooth nanorod arrays. We expect that the air pockets trapped in nanopores will keep the low-friction (or CB mode) regime stable, although more in-depth study is necessary to confirm the air stability. By considering the double roughness features, it would be possible to form self-cleaning or low-friction water flow microchannels.

Acknowledgment. This work was supported by the Korea Research Foundation Grant funded by the Korean Government (MOEHRD, KRF-2005-005-J11902 and KRF-C00050) and the Korea Science and Engineering Foundation (R01-2006-000-10426-0-2006). S.P. thanks the SKKU for start-up funds, and S.K.K. is grateful for support from the Center for Nanotubes and Nanostructured Composites.

Supporting Information Available: Sliding angles of water droplets, surface cleaning with a water droplet, contact-angle measurements on gold plates, and FESEM and TEM images of nanoporous gold nanorods. This material is available free of charge via the Internet at http://pubs.acs.org.

LA7026972